RSC Chemical Biology

ROYAL SOCIETY OF CHEMISTRY

COMMUNICATION

View Article Online
View Journal | View Issue

Cite this: *RSC Chem. Biol.*, 2025, **6**, 1391

Received 27th April 2025,
Accepted 29th July 2025

DOI: 10.1039/d5cb00099h

rsc.li/rsc-chembio

Translocation of penetratin-like peptides involving calcium-dependent interactions between glycosaminoglycans and phosphocholine headgroups of the membrane lipid bilayer

Bingwei He,[a] Sonia Khemaissa,[a] Sébastien Cardon,[a] Rodrigue Marquant,[a] Françoise Illien,[a] Delphine Ravault,[a] Fabienne Burlina,[a] Emmanuelle Sachon,[ab] Astrid Walrant [a] and Sandrine Sagan *[a]

Cell-penetrating peptides (CPPs) can internalize ubiquitously in cells. To explore the specific targeting issue of CPPs, we used glycosaminoglycan (GAG)-binding peptides previously identified in Otx2 and En2 homeoproteins (HPs). The Otx2 sequence preferentially recognizes highly sulfated chondroitin (CS) and the En2 one, heparan sulfates (HS) GAGs. The two HPs internalize in specific cells thanks to their GAG-targeting sequence. We studied the capacity of chimeric peptides containing a GAG-targeting and a penetratin-like sequences to enter into various cell lines known to express different levels and types of GAGs. Since GAGs are found at the vicinity the membrane lipid bilayer, we also analyzed the putative binary and ternary interactions between heparin (HI), (4S,6S)-CS (CS-E), zwitterionic phosphocholine (PC) model membranes and those chimeric peptides. Altogether, our results demonstrate the existence of Ca^{2+}-dependent interactions between GAGs and PC lipid bilayers, the major phospholipid headgroup found in animal cell plasma membrane. In addition, the interaction of CS-E (but not HI), with PC favors the binding of the chimeric CS-E-recognition motif-penetratin-like peptide and its subsequent crossing of the lipid membrane to access directly to the cytosol of cells. Altogether, this study brings further understanding of translocation mechanism of CPPs, which requires specific GAGs at the cell-surface. It also shed light on the role of GAGs in the cell transfer specificity and paracrine activity of HPs.

Introduction

Cell-penetrating peptides (CPPs) are short peptides, typically fewer than 30 amino acids, that can cross cell membranes and deliver a variety of cargoes—including small molecules, proteins, nucleic acids, and nanoparticles—into cells. Penetratin is one of the historically described CPP, being the helix-3 (RQIKIWFQNRRMKWKK) of the homeodomain from the drosophila homeoprotein (HP) *Antennapedia*. HPs are signalling factors transferring between cells and regulating several important cellular functions, including gene transcription and protein translation.

CPPs are known to internalize into all cell types through two main routes concomitantly, endocytosis paths and direct translocation, the latter implying temporary and non-toxic disruption of the lipid bilayer of the plasma membrane.[1] The endocytic ways are quite well understood and involve almost all kinds of reported endocytosis processes,[2] including atypical ones.[3] By contrast, the understanding of translocation is still in its infancy, since this process is difficult to track directly in living cells. Most studies report indeed the use of a temperature below 12 °C (to inhibit endocytosis pathways), or endocytotic inhibitors to highlight translocation in cells. Each of these two methods have their own drawbacks, since lowering the temperature impacts the fluidity and dynamics of the cell membrane, whereas the use of endocytotic inhibitors induces side-effects that are generally overlooked.[4,5] Other studies report the development of methods to study the translocation process only, without using inhibitors or low temperatures.[6,7] Those studies do not address however the mechanism(s) behind, in particular the specific and required cell-membrane partners that are recruited to induce the reversible and temporary disruption of the cell membrane bilayer, the so-called translocation.

Although the membrane lipid content is quite conserved from one animal cell to the other, their cell-surface strongly differs in terms of the extracellular matrix that forms a gel-like microenvironment above the lipid bilayer. The cell-surface is covered in particular with heparan sulfates (HS) and chondroitin sulfates (CS) glycosaminoglycans (GAGs), the long negatively-charged chains of linear and differently sulfated polysaccharides anchored on proteins (proteoglycans). Several studies reported that

[a] *Sorbonne Université, École Normale Supérieure, PSL University, CNRS, Chimie Physique et Chimie du Vivant (CPCV), 75005 Paris, France. E-mail: sandrine.sagan@sorbonne-universite.fr*
[b] *Sorbonne Université, Mass Spectrometry Sciences Sorbonne University, MS3U, Platform, 75005 Paris, France*

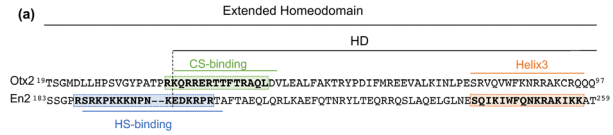

(b)

Peptide name	GAG-targeting	H3	Net charge (+,−)	Average charge per residue
H3		SQIKIWFQNKRAKIKK	+6 (6+, 0−)	0.38
GAG^{En}	RSRKPKKKNPNKEDKRPR		+8 (10+, 2−)	0.44
GAG^{En}-H3	RSRKPKKKNPNKEDKRPR	SQIKIWFQNKRAKIKK	+14 (16+, 2−)	0.41
GAG^{Otx}	RKQRRERTTFTRAQL		+5 (6+, 1−)	0.33
GAG^{Otx}-H3	RKQRRERTTFTRAQL	SQIKIWFQNKRAKIKK	+11 (12+, 1−)	0.35

Fig. 1 (a) Sequence alignment of Otx2 and En2 extended homeodomains. (b) Sequence of the peptides used in this study. All peptides have a carboxamide moiety at the *C*-terminus and contain a biotin-Gly_4 tag at the *N*-terminus except the chimeric peptides GAG^{En}-H3 and GAG^{Otx}-H3 that contain a biotin-Gly_5 tag.

those GAGs are necessary for interactions with and internalization of CPPs in cell model systems[8] or in cells.[1,9–11] Although it is well established that HS proteoglycans are involved in endocytotic pathways of different types of molecules including CPPs,[12,13] whether HS and CS are also involved in translocation[9,10,14] is a question that remains to be addressed and is one objective of the present study.

Whatever the internalization pathway, either by endocytosis or translocation, CPPs internalize ubiquitously in cells. This lack of cell-targeting property hampers the use of these peptides as efficient delivery tools for biotechnological or therapeutic purposes. In contrast, homeoproteins (HPs) are endowed with cell-targeting properties towards specific regions of the brain expressing different levels and types of GAGs.[15] Interestingly, it has been reported that within the sequences of HPs such as En2[16] or Otx2,[17] a GAG-binding sequence upstream of the homeodomain helix-3 is required for the cell-specific internalization of these proteins[17,18] and their function in the central nervous system.[18] The GAG-targeting sequences are a pentadecapeptide, GAG^{Otx} (RKQRRERTTFTRAQL), in Otx2 and an octadecapeptide, GAG^{En} (RSRKPKKKNPNKEDKRPR), in En2 (Fig. 1a). These peptides preferentially recognize chondroitin-4,6-disulfate (CS-E) and highly sulfated HS, respectively.[16,17]

In the present study, we analyzed the ability of the two GAG-targeting sequences, GAG^{Otx} and GAG^{En}, to internalize on their own into cells. We also combined these GAG-targeting peptides with the penetratin-like sequence of En2, to construct putative mini-homeodomain mimics endowed with cell- targeting and internalization and properties (Fig. 1b). With this objective, we used four ovarian cell types that express different levels and types of HS and CS. Wild type chinese hamster ovarian cells (CHO-K1) express HS and chondroitin mono-sulfates (CS-A and CS-C); mutant GAG-deficient ovarian cells (pgsA-745) derived from K1, have genetical defects in xylosyltransferase[19] and express only 5–10% GAGs compared to K1 cells; human ovarian adenocarcinoma cells CaOV-3 overexpress HS and (4,6)-CS (CS-E) subtypes;[20] finally human ovarian adenocarcinoma SKOV-3 cells overexpress CS-E and HS.[21] We examined the impact of GAGs on the internalization of all these peptides in the above-mentioned cell lines. In addition, using a combination of calorimetry (ITC, DSC), fluorescence spectroscopy and dynamic light scattering (DLS), we dissected the bi- and tripartite interactions between GAGs, phospholipids and the chimeric peptides.

Altogether, the results obtained from this combination of analyses, led us to propose a role of cell-surface GAGs in the internalization of the peptides, not only for endocytosis but also for translocation that permits the direct access of the peptides to the cytosol. This study is thus of significant interest to the field of membrane biology and for intracellular delivery purposes.

Results and discussion

Homeoprotein-derived GAG-binding peptides interact differently with HI and CS-E

The group of Prochiantz previously reported a motif upstream the Otx2 homeodomain that interacts preferentially with CS-E, RKQRRERTTFTRAQL.[17] More recently, we identified in En2 another motif that binds highly sulfated HS, RSRKPKKK NPNKEDKRPR.[16] The two motifs are not strictly aligned in the two HP sequences. We designed chimeric peptides formed by the two aforementioned GAG-recognition sequences (GAG^{Otx} and GAG^{En}), extended at the *C*-terminus by the En2 penetratin-like sequence (SQIKIWFQNKRAKIKK) to create minimalistic homeodomain mimics (Fig. 1b).

We first wanted to examine whether all the peptide sequences interact with GAGs. Using isothermal calorimetry (ITC), we determined the binding parameters of the designed peptides with heparin (HI) used as a mimic of highly sulfated HS, or CS-E (Table 1). HI is a highly sulfated polymer, mostly composed of trisulfated Glc(NS,6S)–IdoA(2S), which is found in *N*-sulfated domains of HS,[22,23] a key structure for protein recognition.[24] In contrast, CS-E polymer is a repetition of GlcA-GalNAc(4S,6S) disaccharides.

The two anionic polysaccharides also differ in size. HI (12 kDa) contains about 20 disaccharides and CS-E (72 kDa), about 135 disaccharides. To take into account this difference in length, we determined the dissociation constant of the peptide binding to one disaccharide unit only. The global free energy of binding was thus divided by the number of disaccharide units per heparin ($n \approx 20$) or CS-E chain ($n \approx 135$). The dissociation constant per disaccharide unit was then calculated as $K_d^{app} = e^{\Delta G/nRT}$.

All peptides are positively charged at physiological pH (Fig. 1) and can interact with the negatively charged polysaccharides HI and CS-E. This interaction (Table 1) is enthalpically-driven, indicative of H-bonds and electrostatic interactions. The formation of peptide/GAG complexes is entropically disfavored, likely because of the loss of conformational flexibility of the two interacting partners. At first glance, the favorable enthalpy, recorded during formation of the complexes, is not directly related to the net charge of the peptides, indicating the involvement of other interactions than only electrostatic ones (Fig. S1). The apparent affinity is better for HI than for CS-E for all peptides. Since the HI and CS-E

Table 1 ITC thermodynamics of peptides with 12 kDa heparin (HI) and 72 kDa (4S, 6S)-CS (CS-E). Peptides were titrated with the polysaccharides at 25 °C in 50 mM NaH_2PO_4 (pH 7.4), 100 mM NaCl. Results are shown as mean ± SD (n = 3). To get access to the dissociation constant of the peptide to one disaccharide unit only, the global free energy of binding was divided by the number of disaccharide units per heparin ($n \approx 20$) or CS-E chain ($n \approx 135$). The dissociation constant per disaccharide unit was then calculated as $K_d^{app} = e^{\Delta G/nRT}$

Peptide (net charge)	GAG	Stoichiometry (peptide/GAG)	ΔH (kJ mol^{-1})	$-T\Delta S$ (kJ mol^{-1})	ΔG (kJ mol^{-1})	K_d^{app}/disacch. (mM)
H3 (+6)	HI	14 ± 0.1	−200 ± 14	+156 ± 14	−44	411
	CS-E	41 ± 3	−268 ± 53	+258 ± 40	−10	971
GAG^{En} (+8)	HI	6.0 ± 0.4	−74 ± 4	+36 ± 4	−38	464
	CS-E	50 ± 20	−170 ± 30	+130 ± 9	−40	887
GAG^{otx} (+5)	HI	17 ± 4.7	−28 ± 3	−8.0 ± 3.0	−36	484
	CS-E	100 ± 22	−60 ± 6	+11 ± 2.0	−49	864
GAG^{En}-H3 (+8)	HI	4.5 ± 0.5	−108 ± 2	+66 ± 2.0	−42	429
	CS-E	25.5 ± 5.5	−291 ± 21	+249 ± 19	−42	882
GAG^{Otx}-H3 (+8)	HI	11.5 ± 4.5	−163 ± 3	+117 ± 3.0	−46	395
	CS-E	70 ± 30	−746 ± 96	+693 ± 103	−53	853

disaccharide content varies in terms of sulfation pattern, the measured K_{Ds} should be taken with caution, as they are macroscopic average values. Interestingly, an entropy/enthalpy compensation phenomenon is observed for the formation of the peptide/GAG complexes (Fig. S2).

Overall, the results show that all peptides bind HI and CS-E with slightly different thermodynamic parameters.

Absence of cytotoxicity of the peptides

The peptides were tested for their cytotoxicity in CHO-K1 cells and for hemolysis on red blood cells. Briefly, for the former assay, 5000 CHO-K1 were incubated for 1 h with the peptides up to 20 μM concentration. Untreated cells were defined as positive control while the wells without cells stood as a negative one. For the hemolysis assay, 100 μL red blood cells solution was incubated with peptides at 10 μM or 50 μM for 1 h at 37 °C. As a positive control, complete cell hemolysis was obtained by incubating blood cells with 0.1% Triton X-100. The negative control was obtained by incubation of blood cells with PBS. The release of hemoglobin was measured by photometric absorption at 540 nm. In those conditions (Fig. S3), the peptides have neither cytotoxicity (up to 20 μM) nor hemolytic activities (up to 50 μM).

GAG-binding peptides hardly internalize into cells when the internalization of chimeric peptides, is boosted in the presence of sulfate-containing GAGs

We wanted next to analyze the cell-internalization capacity of the peptides in cell lines expressing different levels and types of HS and CS glycosaminoglycans. Using biotin- and N-terminal deuterium-labeled peptides as internal standards for mass spectrometry (MS) quantification,[25,26] we evaluated, using MALDI-TOF MS, the capacity of the peptides to internalize within one-hour time incubation into different cell lines: CHO-K1, pgsA745, CaOV-3 and SKOV-3, reported to express different contents of HS and CS-E[19–21] (Fig. 2). The MS quantification method is robust and is routinely used to quantify only the intracellular peptide, although it can also be used to measure the membrane-bound one.[26,27] It also permits to detect whether the peptides are degraded intracellularly as lower masses can be observed on mass spectra.[28] We can also check the molecular state (intact or subject to proteolysis) of

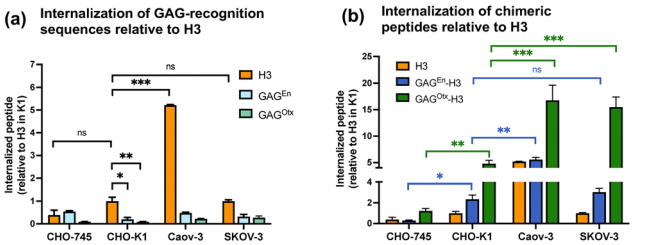

Fig. 2 Quantity of (a) H3 and GAG-binding sequences and (b) chimeric peptides internalized in one million cells after 1 hour incubation with peptides (7 μM) at 37 °C, determined by MALDI-TOF MS.[25,26] The amounts were normalized relative to H3 internalization in K1 cells.

the extracellular peptide in the cell incubation medium. When cells are incubated at 37 °C with peptides, we measured the peptide internalized by both endocytosis and translocation. Cooling down the incubation milieu to 4 °C allows us to discard endocytosis and measured the peptide internalized by translocation only, although it can be underestimated because the membrane fluidity is affected.

H3, GAG^{Otx} and GAG^{En2} peptides were first studied. As expected,[1] the H3 peptide internalizes 3-times less in pgsA-745 compared to K1 and SKOV-3 cells. H3 internalization is however 5-times higher in the CaOV-3 (HS overexpression) than in the CHO-K1 and SKOV-3 cell lines. In contrast, the two GAG-binding peptides are hardly internalized (<0.5 pmoles) in the four cell types (Fig. 2a). This result is important since it shows that although H3, GAG^{En} and GAG^{Otx} all bind HI and CS-E (Table 1), the latter two peptides hardly internalize in cells. It implies that the binding capacity of a peptide to GAGs cannot be used to predict its cell internalization efficacy.

For the H3 peptides, the presence of a GAG-recognition sequence has significant effect on peptide internalization in K1 cells, that is 2-fold and 5-fold higher, respectively for GAG^{En}-H3 and GAG^{Otx}-H3 compared to H3 alone. In addition, internalization of GAG^{En}-H3 is 2-fold higher in CaOV-3 where HS are overexpressed compared to CHO-K1 cells. Finally, GAG^{Otx}-H3 internalization is enhanced about 3-fold in CaOv-3 and SKOV-3 cells that both express higher levels of CS-E compared to CHO-K1 cells.

Altogether these results show that the GAG-binding sequence plays a pivotal role in the chimeric peptides by strengthening both the cell-targeting and internalization efficacy of the peptides.

Impact of the presence of a linker between the GAG-binding motif and the internalization H3 domain on GAG interaction, secondary structure and cell-penetration of peptides

The first chimeric peptides we designed connect directly the GAG-recognition to the cell-penetrating sequence. We further evaluated whether the GAG-binding and the H3 internalization motifs can act at distance, similarly to the homeodomain, or under more conformational flexibility or restriction. We synthesized a series of GAG^{En}-linker-H3 and GAG^{Otx}-linker-H3 analogues with different linker moieties. The linker was either an aminopentanoic acid (Apa, NH_2–$(CH_2)_4$–COOH), an amino-PEG_2-acid (PEG_2, NH_2–$(CH_2$–CH_2–$O)_2$–CH_2–COOH), Pro, Gly or Gly_4. It introduces a space between the GAG-binding motif and the H3 internalization domain of 3 conformationally constrained atoms (Pro) or more flexible 3 (Gly), 6 (Apa), 9 (PEG_2) or 12 atoms (Gly_4).

As seen in Fig. 3, for the GAG^{En}-linker-H3 series, the internalization efficacy was in the best case, GAG^{En}-Apa-H3, similar to the peptide without linker and always significantly decreased for all other analogues. In contrast, for the GAG^{Otx}-linker-H3 series, we could obtain increased internalization for the analogue containing the longer linker (Gly_4, 12 atoms), whereas the 6- and 9 atoms linker-containing analogues have similar internalization efficacy as the reference peptide without linker.

Finally, the analogues containing the 3 atoms-linker (Pro, Gly), have significant decreased internalization compared to the peptide without linker. Altogether these results show that except for the Apa linker that has no impact on the internalization efficacy of the peptides compared to the original one without linker, opposite effects were observed with the different linkers on internalization of GAG^{En}-linker-H3 and GAG^{Otx}-linker-H3 analogues.

The thermodynamics of these peptides interacting with HI or CS-E were therefore also studied by ITC (Table S1). Globally, formation of peptide/GAG complexes is enthalpically-driven for all peptides. We could not find any direct correlation however between the thermodynamics parameters and the capacity of the peptide to internalize into cells.

To examine the role of the secondary structure in those opposite effects on internalization, we next analyzed the whole chimeric peptide series by circular dichroism (CD), each peptide alone or in interaction with HI (used at a saturating concentration previously determined by ITC), or palmitoyl-2-oleoyl-*sn-glycero*-3-phospho-rac-(1-glycerol) (POPG) vesicles. Results (Table S2) indicate that all peptides remain unstructured in 100 mM NaF, 10 mM phosphate buffer. In the presence of HI, the GAG^{Otx}-linker-H3 series is mostly unstructured while the addition of HI increased the peptides propensity to adopt a β-strand structure. In contrast, in the presence of POPG vesicles, at low peptide/lipid (P/L) ratio, the GAG^{Otx}-linker-H3 peptides are both unstructured and α-helical. With increasing P/L ratio, the preferred conformation is random coil and β-strand. The GAG^{En}-linker-H3 series has no structure in 100 mM NaF, 10 mM phosphate buffer. In the presence of HI, these peptides remain principally unstructured and also populate α-helix and β-strand conformations. In the presence of POPG vesicles, the peptides conformational preference is the random coil and slightly the β-strand. Altogether, these results show that these peptides are chameleon-like molecules, adapting their structure according to the interaction partner, as previously reported.[29] Mostly unstructured in solution, they fit to α-helices or β-strands depending on the interaction partner or the stoichiometry of the interaction complex. This finding suggests that depending on the GAG-recognition sequence, the chimeric peptide interacts at the cell-surface with different partners or differently with the same partners, changes its structure accordingly, which results in various modes of internalization efficacy.

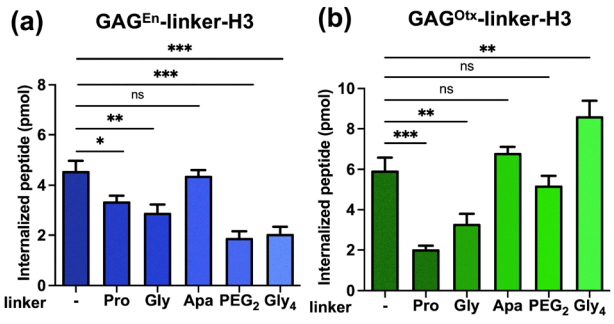

Fig. 3 MALDI-TOF MS quantification (pmol) of internalized GAG^{En}-linker-H3 and GAG^{Otx}-linker-H3 analogues (the linker being either Pro, Gly, Apa, PEG_2 or Gly_4) after incubation at 37 °C with 10 μM peptides with one million CHO-K1 cells.

Affecting the presence and structure of GAGs at the cell-surface impairs peptide entry

To analyze further the role of the negatively-charged cell-surface GAGs, we next examined the effect of enzymatically- or chemically-driven alteration of sulfation of SKOV-3 cell surface GAGs on peptide internalization. We pre-treated cells with heparinases I-III and/or chondroitinases ABC, which hydrolyze GAGs, or sodium chlorate ($NaClO_3$), an inhibitor of GAG sulfation (used at 10 and 100 mM non-cytotoxic concentrations). Results in Fig. 4 indicate that the internalization of GAG^{En}-H3 and GAG^{Otx}-H3 drops when the presence of sulfated GAGs is decreased. The internalization of GAG^{En}-H3 is reduced when cells are pre-treated either by heparinases I-III (64% decrease) or chondroitinase ABC (40% decrease), while in the same experimental conditions, GAG^{Otx}-H3 internalization is only affected by ChABC (38% decrease). The importance of sulfation was confirmed by treating cells with the sulfate adenylyltransferase inhibitor $NaClO_3$. In the latter case, 10 mM $NaClO_3$ decreases by 43% GAG^{Otx}-H3 internalization.

Altogether, the effect of $NaClO_3$ and enzymatically-driven degradation of cell-surface GAGs confirms the role of GAGs in peptide internalization, which was previously reported as the constitutive clathrin- and caveolin-independent endocytic

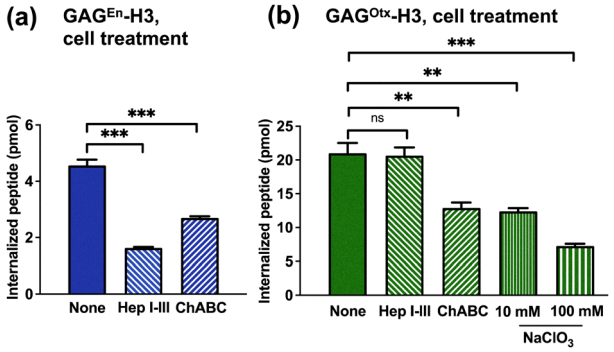

Fig. 4 MALDI-TOF MS quantification of internalized (pmol) chimeric peptides incubated (7 μM) 1 h at 37 °C with one million SKOV-3 cells submitted to GAG hydrolysis (HepI-III, ChABC) or desulfation ($NaClO_3$).

pathway,[30] known to internalize heparan sulfate proteoglycans (HSPGs) and HSPG-binding molecules essential for cell maintenance and signaling.[31,32]

Finally, these results indicate that sulfated cell-surface GAGs are indeed essential for the internalization of the GAG-targeting chimeric peptides. Whether this internalization relates to endocytosis only or also to translocation is a question totally opened that we wanted to address further.

Calcium-dependent interactions of HI and phosphocholine (PC) in model membranes

To get further insight into the role of GAGs in the mechanism of internalization, endocytosis only or also in translocation, we next examined whether those long linear sulfated polysaccharides free or anchored to the cell plasma membrane by a protein core could interact with the lipid bilayer. The presence of GAGs floating above the lipid bilayer make the possibility of their direct contact with the lipid headgroups of the cell membrane very probable. A strong argument for such hypothesis is that the efficient extraction of plasma heparin includes a stringent delipidation step.[33] Concomitant with this latter observation, the zwitterionic phosphocholine headgroup is found as the major plasma HI binding lipid.

Therefore, we next addressed whether GAGs and phospholipids can interact together and the potential consequence of this interaction in the translocation of CPPs, which has not been documented so far.

Since the major phospholipids of the animal cell membrane contain the phosphocholine headgroup, we used large unilamellar vesicles (LUVs) composed of (14 : 0) PC (1,2-dimyristoyl-*sn-glycero*-3-phosphocholine, DMPC), to test by DSC whether HI could modify the thermotropic phase behavior of this phospholipid (Fig. 5). The pre-transition peak of 1,2-dimyristoyl-*sn-glycero*-3-phosphocholine (DMPC), appears around 15 °C, while the main transition is recorded at 25 °C along with an associated enthalpy about 20 kJ mol^{-1}. Addition of increasing amounts of HI in the presence of divalent cations (Mg^{2+}, Ca^{2+}), leads to the gradual increase of the pre-transition and main-transition temperatures, together with an increase of the area of the main phase transition peak (Fig. 5b).

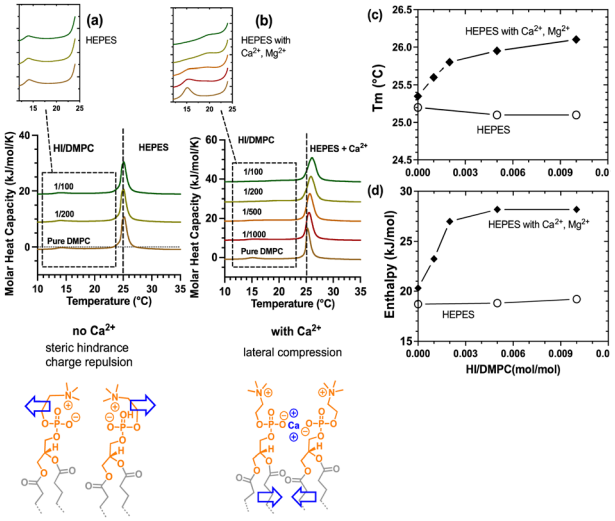

Fig. 5 DSC analysis of T_m and enthalpy changes upon addition of heparin (HI) to 1 mg mL^{-1} DMPC LUVs in (a) HEPES buffer and (b) HEPES buffer plus Ca^{2+}, Mg^{2+}. Curves correspond to DMPC mixed with different amounts of HI. The pre-transition of DMPC is circled by the dashed rectangle and zoomed in the left top; corresponding main phase transition temperature (c) and enthalpy (d) of DMPC LUVs according to HI/DMPC ratio. The thermograms are from one experiment repeated once. Similar results with DPPC and DSPC in SI. Below thermograms (a) and (b) is represented the hypothesis for the impact of Ca^{2+} on PC organization: in the absence of Ca^{2+}, the positively charged choline interacts with the negative phosphate moiety of the polar head, which would create steric hindrance or charge repulsion between the polar head groups of adjacent phospholipids; in the presence of Ca^{2+}, the divalent ion bridging phosphate moieties would allow the choline headgroup to reorientate outside the bilayer and induce lateral compression between adjacent alkyl chains.

By contrast, there is no change in the pre-transition and main transition peaks in the absence of Ca^{2+}, Mg^{2+} even at the maximal ratio (1/100) of HI/DMPC (Fig. 5a), consistently with reports from the literature.[34] The corresponding thermodynamic parameters ΔH and T_m for the different HI/DMPC ratios in the absence (a), or the presence of Ca^{2+}, Mg^{2+} (b), are shown in Fig. 5c and d. These results indicate that HI interacts with the head group of DMPC in the presence of the divalent cations, compresses phospholipid headgroups and leads to reduced hydrophobic forces between alkyl chains. The interaction between alkyl chains of DMPC requires more energy to shift from gel state to fluid phase so that T_m reached 26 °C (Fig. 5c) at the highest HI/DMPC ratio. A similar trend is observed with the phospholipids dipalmitoylphosphatidyl-choline -DPPC or (16 : 0)PC-, and distearoylphosphatidylcholine -DSPC or (18 : 0)PC- (Fig. S4). In the presence of increasing amounts of HI with DPPC LUVs, the pre-transition peak becomes wider before disappearing and T_m shifts to higher temperature (Fig. S4). For DSPC, the pre-transition becomes invisible and the main transition peak is broadened and in contrast to DMPC and DPPC, becomes asymmetrical and splits. Splitting of the peak for DSPC is observed from the 1/500 HI/DSPC ratio and could indicate the formation of flocs and HI-rich and HI-poor vesicles. As for DMPC, the enthalpy increases with the addition of HI to DPPC and DSPC vesicles, showing that HI induces phospholipid compression.

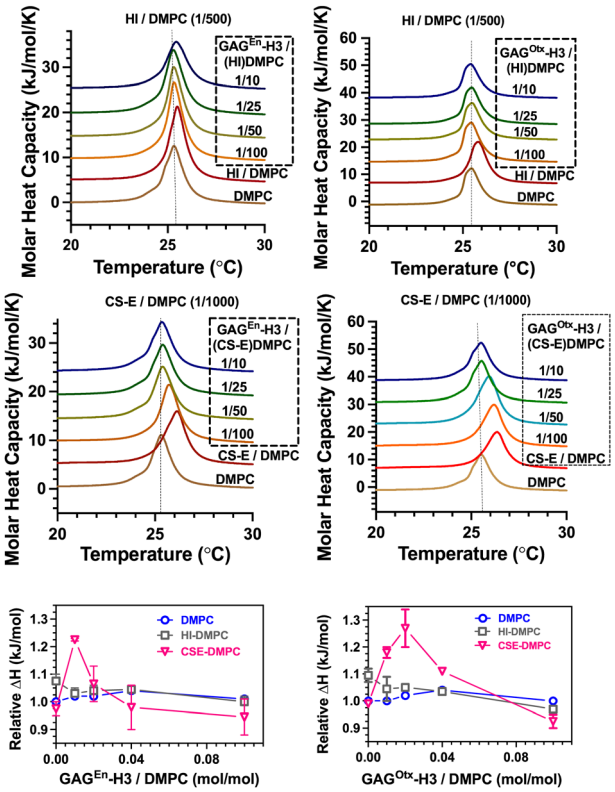

Fig. 6 DSC analysis of enthalpy changes upon addition of GAG^{En}-H3 (a–c) or GAG^{Otx}-H3 (d–f) to 1 mg mL^{-1} HI- (grey) or CSE-decorated (pink) DMPC LUVs in HEPES buffer plus Ca^{2+}, Mg^{2+}. (c) and (f) Curves correspond to the relative ΔH that is the ratio between the enthalpy recorded with GAG-decorated DMPC LUVs and the one with pure DMPC LUVs (blue), according to different ratios of peptide/DMPC LUVs.

Together, these results confirm that in the presence of the divalent cation Ca^{2+}, negatively-charged linear polysaccharides (GAGs) can interact with the phosphocholine lipid bilayer found in the animal cell plasma membrane.

Ternary interactions between GAGs, PC vesicles and peptides

We questioned next how the chimeric peptides, GAG^{Otx}-H3 or GAG^{En}-H3, would impact these interactions between GAGs and PC lipid bilayers.

To do so, we prepared DMPC LUVs decorated with either HI at a ratio of 1/500 or CS-E at a ratio of 1/1000. The positively-charged peptides hardly interact with MLVs of DMPC alone, as previously reported,[35] but both peptides affect the DMPC main transition in the presence of GAGs (Fig. 6a, b, d, e and Fig. S5). The trend is different for HI-decorated LUVs. The relative ΔH curves (Fig. 6c, f and Fig. S5) of DMPC and HI-decorated DMPC LUVs rapidly converge upon the first addition of peptide (ratio = 0.01).

In contrast, GAG^{En}-H3 increases the enthalpy at 0.01 peptide/HI-DMPC ratio before overlaying the DMPC curve afterwards. This observation is emphasized in the case of GAG^{Otx}-H3. With this latter peptide, the enthalpy is increased for the peptide/LUV ratio between 0.01 and 0.04, consistent with the simple adsorption of the peptide at the surface of CS-E-decorated vesicles that results in lipid ordering. At a certain peptide/vesicle threshold (>0.04), the trend reverses with a decrease of enthalpy to reach a value slightly lower than the one measured for LUVs alone (Fig. 6). This observation likely reflects insertion of the peptide between the acyl chains of DMPC.

Altogether, these results indicate that GAG^{Otx}-H3 and to a lesser extent GAG^{En}-H3, can interact with DMPC lipid bilayers covered by anionic GAGs in the presence of calcium divalent cation, more particularly CS-E in the context of this study.

GAG^{Otx}-H3 interacts with phosphocholine in the presence of Ca^{2+}-dependent CS-E-bridge

In the above experiments, we evidenced the existence of ternary interactions between anionic GAGs, zwitterionic PC lipid bilayers and the chimeric peptides. We propose that CS-E could directly interact with the cell membrane and establish a bridge for peptide interaction with the lipid bilayer of the plasma cell membrane.

We further tested this hypothesis by monitoring Trp fluorescence in peptides interacting with model membranes that mimic the cell membrane, as the two chimeric peptides contain one Trp residue in the common H3 segment of their sequence. We analyzed the partitioning of the two peptides within PC LUVs either alone or decorated at their surface by HI or CS-E, as well as their interaction with GAGs alone, considering that binding to a GAG could possibly lead to a change in the Trp environment and thus be accompanied by a shift of the maximum emission wavelength.

As expected, Trp fluorescence intensity increases linearly according to the peptide concentration (Fig. S6). Upon addition of increasing concentrations of DOPC LUVs (Fig. S7), no shift of Trp wavelength emission (λ_{em}) is observed, indicating the absence of modification of the Trp environment, thus reflecting the absence of partitioning of the peptides into PC vesicles in these conditions. By contrast, addition of HI- or CS-E-decorated DOPC LUVs shifted λ_{max} of the Trp-containing peptides to lower wavelengths (Table 2).

This blue shift is classically used as an indicator of a more hydrophobic environment of the Trp residue. This blue shift increases to a maximum of 14–18 nm when GAG^{En}-H3 binds HI or HI-decorated PC vesicles, with an apparent affinity K_d^{app} in the μM range similar in the two cases. In the case of CS-E and CS-E-decorated vesicles, the λ_{max} is shifted by 6–7 nm and the affinity of GAG^{En}-H3 is within the same range for CS-E-decorated vesicles than for CS-E alone, respectively 440 nM and 250 nM. In any case, it appears that GAG^{En}-H3 only interacts with the GAG and does not bind to the PC bilayer.

The peptide GAG^{Otx}-H3 shows a very different behavior in the binding to CS-E and CS-E decorated vesicles (Fig. S8 and Table 2). In both cases, the blue shift increases up to 14 nm but GAG^{Otx}-H3 has a significantly 4-times higher affinity for CS-E-decorated vesicles (130 nM), than for CS-E alone (500 nM).

This observation does not result from disruption/destruction of the vesicles since no calcein leakage could be observed in parallel under the same experimental conditions (Fig. S9).

Table 2 Dissociation constants of GAG^{En}-H3 and GAG^{Otx}-H3 obtained by Trp fluorescence spectroscopy for each peptide binding to HI- and CS-E-decorated DOPC LUVs in the presence of Ca^{2+} and Mg^{2+}, except when specifically mentioned. Values of $(\Delta\lambda)_{max}$ (nm) and K_d^{app} (μM) were obtained from the fits of fluorescence data given in Fig. S7. NA: not applicable

Experimental condition	Measured parameters	GAG^{En}-H3		GAG^{Otx}-H3		
		No lipids	+ DOPC	No lipids	+ DOPC	+ POPG
No GAG	$(\Delta\lambda)_{max}$	—	0	—	0	14 ± 0.5
	K_d^{app}		NA		NA	0.21 ± 0.05
HI	$(\Delta\lambda)_{max}$	14 ± 5.3	18 ± 1.2	15 ± 1	14 ± 1.1	—
	K_d^{app}	5.3 ± 1.2	6.1 ± 1.3	3.3 ± 0.6	3.3 ± 0.4	
CSE	$(\Delta\lambda)_{max}$	6 ± 0.5	7 ± 0.5	14 ± 1.1	13 ± 0.6	—
	K_d^{app}	0.25 ± 0.08	5.3 ± 1.2	0.5 ± 0.13	0.13 ± 0.03	
CSE (no Ca^{2+})	$(\Delta\lambda)_{max}$	—	—	14 ± 0.5	14 ± 1.2	—
	K_d^{app}			0.39 ± 0.05	0.49 ± 0.14	

Interestingly, the binding parameters (blue shift and affinity) for CS-E-decorated vesicles and POPG vesicles are in the same range (Fig. S8 and Table 2). In addition, in the absence of Ca^{2+}, the affinity of GAG^{Otx}-H3 is in the range of 500 nM both for CS-E or CS-E-decorated DOPC. Altogether, these results strongly support an interaction of the peptide with DOPC lipid bilayers, only in the presence of CS-E and calcium. Finally, the peptide has similar binding parameters to HI or HI-decorated PC vesicles.

Altogether, these results evidence that in the presence of Ca^{2+}, CS-E-decorated PC vesicles can mimic negatively charged phospholipid bilayers that positively-charged CPPs are known to insert into. These properties are not shared by HI which was used herein as a HS mimic. These results also highlight the difference of behavior between GAG^{En}-H3 and GAG^{Otx}-H3. In the conditions used herein, the chimeric peptide GAG^{En}-H3 has no discriminating ability to bind to PC lipid bilayers in the presence of GAGs. On the contrary, GAG^{Otx}-H3 has the selective ability to bind CS-E-decorated PC vesicles. CS-E lying on top of PC might be assimilated therefore as a "polar negatively charged headgroup" in CS-E-decorated DOPC vesicles. This observation supports the involvement of CS-E and calcium interactions with the lipid bilayer of cells for GAG^{Otx}-H3 translocation mechanism.

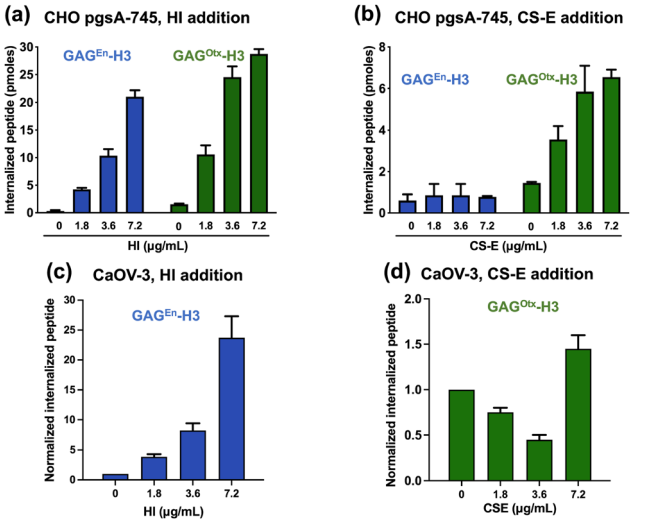

Fig. 7 MALDI-TOF MS quantification internalized GAG^{En}-H3 or GAG^{Otx}-H3 in pgsA-745 (a) and (b) or CaOV-3 (c) and (d) cells, incubated (7 μM) in the absence or presence of various concentrations of HI (a) and (c) or CS-E (b) and (d). In panels (a) and (b), the quantity of internalized peptides is given in pmoles; in panel (c) and (d), the internalization of the peptide in the presence of HI or CS-E is given relatively (normalized), to the quantity measured in the absence of the exogenously added GAGs.

CS-E improves selectively translocation of GAG^{Otx}-H3 in cells

To study whether these ternary interactions may also occur in cells and impact the internalization of the peptides, in particular the translocation process, we analyzed the effect of exogenous HI or CS-E on the internalization efficacy of the chimeric peptides. We first worked with pgsA-745 CHO cells deficient in HS and CS,[19] and incubated these GAG-deficient cells with a mixture of HI or CS-E and the chimeric peptides.

As shown in Fig. 7a, incubation of GAG-deficient cells with each of the peptides in the presence of increasing HI concentrations boosts the quantity of their uptake. At the maximal HI concentration tested (7.2 μg mL^{-1}), about 20 pmoles of GAG^{En}-H3 and 30 pmoles of GAG^{Otx}-H3 are internalized after 1 h incubation with cells. The situation is very different with CS-E (Fig. 7b). On the one side, addition of increasing concentrations of exogenous CS-E does not modify the quantity of GAG^{En}-H3 internalized within 1 h incubation with cells. On the other side, the addition of exogenous CS-E significantly boosts the quantity of internalized GAG^{Otx}-H3. At the maximal CS-E concentration tested (7.2 μg mL^{-1}), the quantity of GAG^{Otx}-H3 inside cells is roughly 5-times greater than in the absence of CS-E.

To understand the processes behind these observations, we determined in parallel the size (obtained from dynamic light scattering experiments) and charge surface (measured through determination of the zeta potential) of the peptide/GAG complexes (Fig. S10). No major difference in the size of the complexes is measured at the highest concentrations of HI or CS-E. The size of HI/GAG^{En}-H3 and CS-E/GAG^{En}-H3 complexes is about 150 and 170 nm, respectively. The size of HI/GAG^{Otx}-H3 and CS-E/GAG^{Otx}-H3 complexes is about 260 and 170 nm, respectively. All complexes have a positive zeta potential.

Therefore, the size and charge of all GAG/peptide complexes are not different from each other and cannot explain the difference observed in peptide internalization in the presence of exogenous GAGs. One plausible but still hypothetical

explanation is that HI/peptide complexes could internalize by endocytosis into GAG-deficient cells while CS-E could selectively improve direct translocation of GAG^{Otx}-H3 only.

To test further this hypothesis, we used CaOV-3 cells for which an overexpression of both HS and CS-E has been reported.[20] In these cells, exogenous HI improves the internalization of GAG^{En}-H3 (Fig. 7c), while addition of exogenous CS-E decreases the quantity of GAG^{Otx}-H3 in cells (Fig. 7d). These data might indicate that the endocytosis route for HI/GAG^{En}-H3 complexes is active, although reduced (2- to 3-folds compared to GAG-deficient cells, not shown), with limited competition with cell-surface endocytosis-supporting GAGs. By contrast, GAG^{Otx}-H3 internalization is significantly slightly decreased in the presence of CS-E, suggesting that the exogenously added CS-E could compete with the cell-surface CS-E to interact with the peptide.

At 7.2 μg mL^{-1} CS-E this competition no longer occurs. These results strongly suggest first that in these CaOV-3 cells, exogenously added CS-E could not interact with the lipid bilayer, likely because the CS-E expressed at the cell-surface already covers the lipid bilayer.

Together, these results need further investigation but reinforce the idea that the cell-surface CS-E can form a bridge that allows the specific-recognition by GAG^{Otx}-H3 peptide, promoting its interaction with the lipid bilayer and its translocation across the plasma membrane of the cells.

Experimental

Materials

Standard *tert*-butyloxycarbonyl (Boc) protected L-amino acids, 4-methylbenzhydrylamine resin (0.54 mmol g^{-1}) and 2-(1*H*-benzotriazol-1-yl)-1,1,3,3-tetramethyluronium hexafluorophosphate (HBTU), hexahydro-2-oxo-1*H*-thieno[3,4-*d*]imidazole-4-pentanoic acid (D-biotin) were purchased from IRIS Biotech GmbH (Marktredwitz, Germany), glycine-*N*-*t*-BOC (2,2-D_2, 98%) was obtained from Cambridge Isotope Laboratories (Andover, MA). Dimethylformamide (DMF), trifluoroacetic acid (TFA), dichloromethane (DCM), diisopropylethylamine (DIEA), acetonitrile (ACN), and piperidine were obtained from Carlo Erba (France). Hydrofluoric acid (HF) was obtained from GHC Gerling Holz & Co. (Germany) and was installed in an HF Teflon apparatus (Toho, Japan). 5-(Boc-amino)pentanoic acid (Apa) and 5-carboxy-fluorescein (FAM) were obtained from BaChem (Switzerland). Anisole, dimethyl-sulfide, α-cyano-4-hydroxycinnamic acid (CHCA), heparinase I, heparinase II, heparinase III, chondroitinase ABC and dioleoyl phosphatidylcholine (DOPC) were bought from Sigma-Aldrich (US). Streptavidin-coated magnetic beads (Dynabead® M-280 streptavidin or Dynabead® MyOne streptavidin C1) were bought from Invitrogen. 1-Palmitoyl-2-oleoyl-*sn-glycero*-3-phosphocholine (POPC) was purchased from Avanti Polar Lipids (USA). Phospholipids 1,2-dimyristoyl-*sn-glycero*-3-phosphocholine (DMPC), 1,2-dipalmitoyl-*sn-glycero*-3-phosphocholine (DPPC),1,2-distearoyl-*sn-glycero*-3-phosphocholine (DSPC), and 1-palmitoyl-2-oleoyl-*sn-glycero*-3-phospho-(1′-rac-glycerol) (sodium salt, POPG), were purchased from Genzyme (Switzerland). Cell lines (CHO-K1, pgsA745, CaOV-3 and SKOV-3) were all from the American Type Culture Collection (ATCC). Cell-counting kit-8 (CCK-8) was obtained from Dojindo Laboratories (Japan).

Peptide synthesis

The peptides H3, GAGs-binding motifs GAG^{Otx} and GAG^{En} were assembled on a 0.2 millimolar scale by using the stepwise tBoc solid-phase synthesis strategy using HBTU as a coupling reagent. After synthesis of the peptide sequences, the peptides on resin were divided into three groups, two of which were respectively elongated by either four non-deuterated (H-peptide) or four deuterated (^{2}H-peptide) glycine residues followed by addition of biotin. Biotinylated [^{1}H]peptides and [^{2}H]peptides were cleaved from the resin by treatment with anhydrous HF (2 h, 0 °C) in the presence of scavenger anisole (1.5 mL per g peptidyl resin) and dimethyl sulfide (0.25 mL per g peptidyl resin). Cleaved peptides were precipitated in diethyl ether and then dissolved in 10% acetic acid. The crude peptides were lyophilized and further purified by preparative reverse-phase HPLC on a C18 column with a linear increasing acetonitrile (ACN) gradient in an aqueous solution containing 0.1% (v/v) TFA. The purity of peptide was more than 95% according to the analytical HPLC evaluation. 1 μL purified peptide solution was mixed with 1 μL 10 mg mL^{-1} CHCA matrix and subsequently verified by MALDI-TOF mass spectrometry (Voyager DE-PRO, Applied Biosystems). Chimeric peptides GAG^{Otx}-H3 and GAG^{En}-H3 were obtained from the peptide synthesis facility (Christophe Piesse, Sorbonne Université, Paris, France; **https://www.ibps.sorbonne-universite.fr/en/core-facilities/pe/peptide-synthesis**).

Liposome preparation

Phospholipids were dissolved into chloroform for the preparation of 1 mg mL^{-1} large unilamellar vesicles (LUVs). Chloroform was evaporated by slow N_2 flow with quick rotation to prepare a homogenous lipid white film on the glass tube wall. The rest of chloroform was further removed completely in a vacuum chamber for 2 h. Films were then hydrated by the addition of 1 mL 10 mM HEPES buffer containing 150 mM NaCl, 2 mM $CaCl_2$, 1 mM $MgCl_2$ and mix strongly under vortex for 10 s to complete the dissolution of lipid films. The obtained multi-lamellar vesicles (MLVs) were then subjected to five freeze-thawing cycles at a temperature above the main transition temperature. Then LUVs are collected after 15-times extrusion of the homogenous lipid suspension filtered through a 100 nm Nuclepore™ track-etch polycarbonate membrane (Whatman, UK) by a mini extruder (Avanti Lipids, Alabaster, AL) at a temperature above the T_m of the lipids.

Isothermal titration calorimetry (ITC)

ITC experiments were performed at 25 °C with a nano-ITC microcalorimeter (TA Instruments, New Castle, DE, USA). Peptides and GAGs were prepared in 10 mM HEPES containing 150 mM NaCl, 2 mM $CaCl_2$ and 1 mM $MgCl_2$ (pH = 7.4). 10 μL aliquots of polysaccharides (HI or CS-E) solution were automatically injected into the 1 mL cell chamber containing

peptide or lipids solution at intervals of 5 min and 250 rpm stirring speed. Peptides and polysaccharide solutions were used at different concentrations relying on the peptide sequence and GAG species (varying between 15 and 80 μM for the peptides, 5 and 100 μM for the polysaccharides). Equivalent HI or CS-E alone was injected into the HEPES buffer for baseline correction. Control experiments were recorded to evaluate the dilution heat of injected solution in buffer solution alone. Experimental raw data were integrated as the amount of heat generated per second during titration and fitted to a theoretical single-binding site titration curve. The thermodynamic parameters were subsequently determined by NanoAnalyze software provided by TA Instruments. Experiments were repeated at least 2 times independently.

Differential scanning calorimetry (DSC)

DSC experiments were performed with a high-sensitivity calorimeter (TA Instruments) through spectra of successive heating and cooling scans (1 °C min^{-1}) of 300 μL of 1 mg mL^{-1} liposomes. Nine scans were obtained for each set and each scanning spectrum should be basically identical. There was a 10-min interval between each scan to allow thermal equilibration. Peptides or GAGs are added stepwise to liposomes to obtain peptides/lipids molar ratios of 1/100, 1/50, 1/25 and 1/10 or GAGs/lipids molar ratios of 1/1000, 1/500, 1/200, 1/100 in each set of scans. The scan of HEPES was conducted as blank for baseline correction. Parameters of pre-transition temperature (pre-T_m), main transition temperature (T_m) and heat capacity change ΔH (the main transition peak area) were analyzed by the fitting program NanoAnalyze provided by TA Instruments. Five to six heating and cooling scans in each set were performed.

Dynamic light scattering (DLS) measurements

The size and zeta (ζ) potential of the peptide/GAG complexes was determined by DLS. Peptide and GAGs were mixed at the indicated concentrations, that is one peptide and GAGs (HI or CS-E), were added to 250 μL MQ water to form final 7.5 μM peptide and 1.8 μg mL^{-1} or 7.2 μg mL^{-1} GAG. Hydrodynamic diameters and ζ-potential of the complexes were measured by using a Zetasizer Nano ZS apparatus (Malvern Instruments, United Kingdom).

Trp fluorescence measurements

Tryptophan (Trp) fluorescence emission spectra were monitored by a fluorometer mentioned above. The excitation wavelength of Trp is 280 nm and the corresponding spectra from 300 and 420 nm are recorded. Acquisition duration of 0.5 s/1 nm twice was conducted. Concentrations of 10, 20, 30, 40, 50 μM peptides were prepared in 100 μL 10 mM HEPES buffer (150 mM NaCl, 2 mM $CaCl_2$ and 1 mM $MgCl_2$, pH 7.4) and their fluorescence intensity was measured as a standard peptide dilution curve. 20 μM peptide was titrated by stepwise addition of 10 μM CS-E or 80 μM HI in HEPES buffer. The fluorescence intensity of each titration was corrected by taking into account the peptide dilution. Raw spectra were smoothed by Prism GraphPad (10 neighbor points), the fluorescence intensity and maximal emission wavelength were subsequently obtained. The nonlinear titration fit was plotted by the maximal emission wavelength change $\Delta\lambda_{max}$ according to the corresponding GAG concentration. The K_d^{app} was determined with Prism one site-specific binding. For GAG modified LUVs, firstly 40 mM DOPC LUVs (or POPG LUVs) and 10 mM DOPC LUVs were prepared in HEPES buffer, then 80 μM HI was added to 40 mM DOPC LUVs (1/500) or 10 μM CS-E was added to 10 mM DOPC LUVs (1/1000) for 15 min incubation at room temperature to form GAG modified LUVs. Finally, 20 μM GAG^{En}-H3 and GAG^{Otx}-H3 were titrated by GAGs-decorated LUVs respectively and the spectra were analyzed as described above. GAG^{Otx}-H3 was also titrated by CS-E and CSE-decorated DOPC in 10 mM HEPES buffer containing 150 mM NaCl without Ca^{2+} or Mg^{2+}. The experiment was repeated independently at least two times.

Cell culture

Wild type Chinese Hamster Ovary (CHO-K1) cells and GAGs-deficient mutant pgsA-745 cells which lack the xylosyltransferase needed for glycosaminoglycan (GAG) synthesis were grown in Dulbecco's modified Eagle's medium F-12 (DMEMF-12) with L-glutamine and 15 mM HEPES. HEK cells and HeLa cells were grown in DMEM with 4.5 g L^{-1} D-glucose and pyruvate. Two types of human ovarian cancer cell lines CaOV-3 and SKOV-3 were cultured in DMEM with Glutamax and McCoy's 5A medium respectively. All complete culture medium was supplemented with 10% fetal bovine serum, penicillin (100 000 IU L^{-1}), streptomycin (100 mg L^{-1}). Cells were grown in a humidified atmosphere at 37 °C and 5% CO_2.

Cell treatments

Cells need to be treated before peptide incubation. For GAGs sulfation removal, sodium chlorate was added to the medium to obtain 10 μM or 100 μM concentrations along with SKOV-3 cells seeding on a 12-well plate for 24 h. Cells were then incubated with peptides (7.5 μM) for 1 h. As for GAGs degradation, 500 μL 2 U mL^{-1} chondroitinase ABC (ChABC) or heparinase I II III in Tris buffer (50 mM Tris, 60 mM sodium acetate trihydrate, 0.02% BSA, pH 8) are prepared and incubated with cells for 2 h at 37 °C, then cells are gently washed with HBSS for three times. Peptides in 500 μL DMEM were incubated with cells and treated immediately with supplementation of exogenous GAGs for 1 h incubation. Exogenous HI fragments were obtained by heparinases pretreatment 10 min at 37 °C and then were added to the cells with peptides together.

Quantification peptide cellular uptake by MALDI-TOF MS

Cellular uptake was quantified MALDI-TOF MS. Briefly, this protocol requires isotope-labeled (deuterated glycines are present as a spacer between the peptide sequence and the N-terminal biotin) and unlabeled peptides: biotinyl-[^{1}H]G_4-peptide, biotinyl-[^{2}H]G_4-peptide. Biotin was used to capture peptides in cell lysate with streptavidin-coated magnetic beads. The deuterated peptides were used as internal standard for the absolute measurement of internalized non-deuterated peptides.

10^6 cells per well, seeded 24 h before the experiment in 12-well plates, were incubated with the biotinyl-[^{1}H]G_4peptide (7.5 μM) in serum-free DMEM F-12 medium for 60 min at 37 °C. After incubation and washes, the remaining membrane-bound ^{1}H-peptides were hydrolyzed by trypsin (37 °C). 100 μL 5 mg mL^{-1} soybean trypsin inhibitor (Calbiochem) and 1 mg mL^{-1} bovine serum albumin (BSA) was added to stop digestion. The cells were then washed by 1 mL 50 mM Tris buffer containing 0.1 mg mL^{-1} BSA and lysed in 150 μL lysis buffer containing 0.3% Triton, 1 M NaCl, pH 7.4 and a known amount of the biotinyl-[^{2}H]G_4-peptide. The cell lysate is then immediately boiled at 100 °C for 15 min. The cell lysate is then incubated with C1 streptavidin-coated magnetic beads for 75 min to capture both non-deuterated and deuterated peptides. Peptides are eluted from the streptavidin-coated magnetic beads by addition of CHCA matrix (acidic pH) and spotted on the MALDI plate. Samples are analyzed in positive ion mode with MALDI-TOF on a Voyager-DE Pro mass spectrometer (Applied Biosystems, Foster City, CA, USA) in linear mode (chimeric peptides) or reflector mode (En2H3, GAG-binding peptides). For the linear mode, the MS parameters were optimized as: Accelerating voltage 25000 V; Grid voltage: 95%; Extraction delay time: 350 ns. The absolute quantities of peptide were calculated through the ratio of the peak area corresponding to the non-deuterated and deuterated peptides. The molecular weight of three chimeric peptides being high, reflector mode was not appropriate since peptides were not detected. Therefore, linear mode which is a low-resolution mode was required. The ratio of peaks areas was determined *via* Data Explorer and the quantification software we developed.[16] To be accurate, the quantification of cellular internalization requires working with an identical number of cells under different experimental conditions. Live cells are counted (trypan blue), after incubation with the peptides. The intact molecular state of the peptide in the cell incubation milieu can also be checked by MALDI-TOF MS. For every experiment, we performed triplicate wells.

Conclusions

With this study, we bring further clues for the complex mechanism of internalization of CPPs derived from HPs. CPPs are known to internalize ubiquitously in any cell type, which is a major drawback for their applications in therapeutics or diagnostics. We and others recently identified within HPs, GAG-targeting sequences upstream the penetrating H3 domain.[16,17] We have characterized herein the potency of these sequences to endow CPPs with cell-targeting properties. No linker in the series we introduced between the GAG-targeting sequence and the CPP one was found to improve cell internalization of the peptide. These peptides could be of major interest to develop diagnostic or therapeutic tools since they can target various cancer types where an overexpression of certain types of GAGs has been characterized. The deregulation of both HS and heparan sulfate proteoglycans are involved indeed in many different solid tumors and considered as good targets to treat cancers.[36] The same applies for overexpression of CS for which the sulfation pattern is affected and impact the development and evolution of ovarian cancers for example.[37]

In addition to cell-targeting properties, we moved one step forward in the mechanism of internalization involving GAGs at the cell-surface.

CPPs enter cells through two major internalization pathways, endocytosis and translocation. Depending on their amino acid content and sequence, these peptides, often cationic and containing hydrophobic residues, can indeed interact with various partners at the cell-surface which are differently competent for their internalization.[38,39]

Whatever the route of internalization, these peptides first meet the glycocalyx surrounding cells. The major components of the glycocalyx are HS and CS GAGs and the thickness of the glycocalyx might be 50 to 100 times larger than that of the cell membrane phospholipid bilayer.[40] HS and CS are ubiquitously present in proteoglycans and are long linear and hydrophilic polymers of hundreds to thousands of disaccharide units that carry strong negative charge thanks to the presence of sulfate groups. HS and CS vary from one cell type to the other in terms of sulfation level and position.

Our results indicate that GAGs are important promoters for peptide internalization in cells, but also that GAG-recognition is not sufficient to internalize inside cells. On their own, the GAG-targeting sequences are indeed hardly internalized into cells compared to the cell-penetrating peptide derived from the third helix of En2 HP. Interestingly, the chimeric peptides combining the GAG-recognition and the cell-penetration motifs have internalization efficacy modulated by the type of GAGs present at the cell-surface. The use of heparinases or chondroitinases confirms the role of GAGs in the internalization of both GAG^{En}-H3 and GAG^{Otx}-H3. However, the identification of the relative contribution of HS and CS in the mechanisms of entry of the peptides is biased by the impossibility to prove the partial or total removal from the cell surface of the GAGs specifically targeted by these enzymes. As it was reported that CHO cells do not contain the sulfotransferases required to produce sulphated glycolipids or sulfated N- or O-glycans,[41] sodium chlorate led to undersulfation of proteoglycans and glycosaminoglycans such as heparan sulfate within cells. In those conditions, we confirmed the implication of sulfated polysaccharides in the internalization process.

Regarding the internalization pathways, GAGs are already known to be involved in constitutive clathrin- and caveolin-independent endocytic pathway,[30] and HSPGs are primary receptors for many ligands essential for cell signaling.[31,32]

Apart from these endocytosis pathways, it has been demonstrated *in vitro* that HI can interact with PC. Interestingly, this interaction, most likely between the quaternary ammonium group of the polar head group of the phospholipid and the sulfate group of the GAG, switches the physico-chemical properties of HI. HI is indeed insoluble (98.5%) in chloroform while in interaction with PC, HI becomes essentially soluble (74%) in this solvent.[33]

In addition, it has been reported that in the presence of Ca^{2+}, the anionic phosphate group is far enough from the cationic polar head of PC, and deeply embedded in the bilayer.[42] Ca^{2+} likely acts as a counter-ion of the negatively charged phosphate groups of PC lipids found in the membrane bilayer. When calcium ions are removed, the quaternary ammonium headgroup of the phospholipid likely reorientates to interact with the phosphate, and is no longer available for interactions with endogenous GAGs. In this situation, the steric hindrance and charge repulsion between adjacent phospholipids likely lead to repulsion between phospholipids and to looser bilayer organization.

Other studies have brought evidence that the same type of interaction occurs between CS and PC in the presence of Ca^{2+}.[43–45] Interestingly, Satoh and collaborators found in particular that CS chains of proteoglycans adhere to the surface of the PC membrane while HS chains stretch outward from the membrane surface. Moreover, CS contributes to the formation of PC microdomains in the outer leaflet of the cell membrane.[44]

In our study, we also showed in model systems that both HI and CS-E can interact with PC, only in the presence of Ca^{2+}. However, only the chimeric peptide targeting CS-E (GAG^{Otx}-H3) was able to bind CS-E decorated PC vesicles and showed increased translocation in GAG-deficient cells in the presence of exogenous CS-E. This process does not lead to the formation of permanent and big holes within the bilayer, since we did not observe calcein leakage with model membranes. In agreement, when we used CS-E enriched CaOV-3 cells, the addition of exogenous CS-E competed with cell-surface ones and prevented GAG^{Otx}-H3 entry through translocation.

GAGs at the cell-surface have specific location and topology. CS that are closer to the lipid bilayer, can interact with the choline headgroup of the lipid bilayer and spread out on the cell-surface. On their side, HS stretch outward the cell-surface. We may assume that cationic peptides first meet HS at the cell-surface. Peptides with a CS-recognition motif can then transfer to CS to interact finally with the lipid bilayer, intercalate within the acyl chains and translocate within the cytosol. One plausible hypothesis to explain this transfer, which implies binding from a negatively charged polysaccharide to another, relies on the difference of binding kinetics between solution and membrane-bound partners. Huang *et al.* have recently reported that interaction with supported-partners can be one order of magnitude faster than with partners in solution.[46] Altogether, this study highlights the possibility to endow CPPs with cell specific entry (Fig. 8), and importantly likely through GAG-assisted translocation, by adding a peptide motif that specifically recognizes a CS motif bound at the cell-surface. This finding opens new perspectives for the development of therapeutical or biotechnological applications using CPPs, as well as for the elucidation of the role of GAGs in the paracrine activity and cell transfer specificity of HPs.

Altogether, our study highlights the Ca^{2+}-dependent capacity of negatively-charged GAGs to interact with PC membranes and their role in the translocation process of positively-charged cell-penetrating peptides.

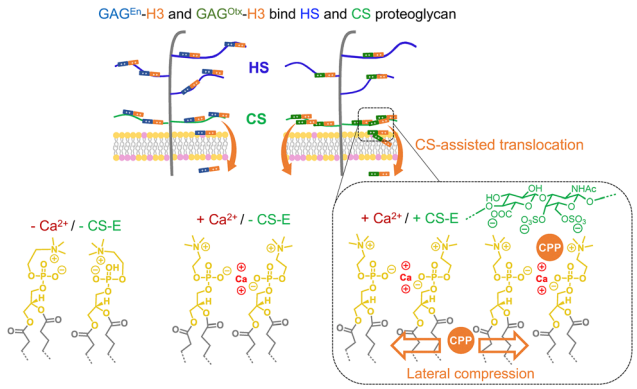

Fig. 8 Schematic representation of the proposed role of GAGs in the internalization mechanism of the chimeric peptides studied herein: GAG^{Otx} and GAG^{En}, H3 and chimeric GAG^{Otx}-H3 and GAG^{En}-H3. CS are located at the vicinity of the lipid bilayer while HS are more distal. The chimeric CPPs bind to HS- and CS- proteoglycans (CS-E bind PC lipids in the presence of Ca^{2+}, leading to an overall anionic complex). Therefore, there are no longer repulsion forces between the cationic choline headgroup and the cationic peptide, could then insert deeper into the lipid bilayer to cross it.

Author contributions

A. W. and S. S. designed research; B. H., S. K., S. C., F. I. and D. R. performed research; R. M., F. B. contributed reagents and E. S., analytical tools; B. H., S. K., A. W. and S. S. analyzed data; A. W. and S. S. wrote the paper.

Conflicts of interest

There are no conflicts to declare.

Data availability

Data supporting the findings of this study not found within the main text of the paper can be found in the SI and upon request.

Fig. S1–S10 and Tables S1 and S2. See DOI: **https://doi.org/10.1039/d5cb00099h**

Acknowledgements

The authors thank the MS3U facility for valuable assistance with MS quantification. Research reported in this publication was supported by the Agence Nationale de la Recherche (ANR) under award number ANR-20-CE44-0018 and by the Chinese Scientific Council (CSC) PhD grant for B.H.

References

1 C. Y. Jiao, D. Delaroche, F. Burlina, I. D. Alves, G. Chassaing and S. Sagan, *J. Biol. Chem.*, 2009, **284**, 33957–33965.
2 I. Ruseska and A. Zimmer, *Beilstein J. Nanotechnol.*, 2020, **11**, 101–123.

3 E. Trofimenko, Y. Homma, M. Fukuda and C. Widmann, *Cell Rep.*, 2021, **37**, 109945.
4 A. I. Ivanov, *Methods Mol. Biol.*, 2008, **440**, 15–33.
5 D. Vercauteren, R. E. Vandenbroucke, A. T. Jones, J. Rejman, J. Demeester, S. C. De Smedt, N. N. Sanders and K. Braeckmans, *Mol. Ther.*, 2010, **18**, 561–569.
6 I. Amblard, E. Dupont, I. Alves, J. Miralves, I. Queguiner and A. Joliot, *J. Cell Sci.*, 2020, **133**, jcs244327.
7 F. Illien, Z. Bánóczi and S. Sagan, *ChemBioChem*, 2024, **25**, 1–7.
8 J. Pae, L. Liivamägi, D. Lubenets, P. Arukuusk, Ü. Langel and M. Pooga, *Biochim. Biophys. Acta, Biomembr.*, 2016, **1858**, 1860–1867.
9 C. Bechara, M. Pallerla, Y. Zaltsman, F. Burlina, I. D. Alves, O. Lequin and S. Sagan, *FASEB J.*, 2013, **27**, 738–749.
10 C. Bechara, M. Pallerla, F. Burlina, F. Illien, S. Cribier and S. Sagan, *Cell. Mol. Life Sci.*, 2015, **72**, 809–820.
11 Y. Takechi-Haraya and H. Saito, *Curr. Protein Pept. Sci.*, 2018, **19**, 623–630.
12 H. C. Christianson and M. Belting, *Matrix Biol.*, 2014, **35**, 51–55.
13 E. Mandarini, E. Tollapi, M. Zanchi, L. Depau, A. Pini, J. Brunetti, L. Bracci and C. Falciani, *Int. J. Mol. Sci.*, 2020, **21**, 1–13.
14 M. E. Favretto, R. Wallbrecher, S. Schmidt, R. Van De Putte and R. Brock, *J. Controlled Release*, 2014, **180**, 81–90.
15 A. A. Di Nardo, J. Fuchs, R. L. Joshi, K. L. Moya and A. Prochiantz, *Physiol. Rev.*, 2018, **98**, 1943–1982.
16 S. Cardon, Y. P. Hervis, G. Bolbach, C. Lopin-Bon, J.-C. C. Jacquinet, F. Illien, A. Walrant, D. Ravault, B. He, L. Molina, F. Burlina, O. Lequin, A. Joliot, L. Carlier and S. Sagan, *Nat. Commun.*, 2023, **14**, 1998.
17 M. Beurdeley, J. Spatazza, H. H. C. Lee, S. Sugiyama, C. Bernard, A. A. Di Nardo, T. K. Hensch and A. Prochiantz, *J. Neurosci.*, 2012, **32**, 9429–9437.
18 A. Joliot and A. Prochiantz, *Front. Cell Dev. Biol.*, 2022, **10**, 1–9.
19 J. D. Esko, T. E. Stewart and W. H. Taylor, *Proc. Natl. Acad. Sci. U. S. A.*, 1985, **82**, 3197–3201.
20 J. P. Connor, M. Felder, A. Kapur and N. Onujiogu, *BMC Cancer*, 2012, **12**, 176.
21 M. J. E. Vallen, S. Schmidt, A. Oosterhof, J. Bulten, L. F. A. G. Massuger and T. H. Van Kuppevelt, *PLoS One*, 2014, **9**, 1–10.
22 M. Maccarana, Y. Sakura, A. Tawada, K. Yoshida and U. Lindahl, *J. Biol. Chem.*, 1996, **271**, 17804–17810.
23 J. E. Turnbull and J. T. Gallagher, *Biochem. J.*, 1991, **277**, 297–303.
24 U. Lindahl, M. Kusche-Gullberg and L. Kjellen, *J. Biol. Chem.*, 1998, **273**, 24979–24982.
25 F. Burlina, S. Sagan, G. Bolbach and G. Chassaing, *Angew. Chem., Int. Ed.*, 2005, **44**, 4244–4247.
26 F. Burlina, S. Sagan, G. Bolbach and G. Chassaing, *Nat. Protoc.*, 2006, **1**, 200–205.
27 S. Aubry, B. Aussedat, D. Delaroche, C. Y. Jiao, G. Bolbach, S. Lavielle, G. Chassaing, S. Sagan and F. Burlina, *Biochim. Biophys. Acta, Biomembr.*, 2010, **1798**, 2182–2189.
28 D. Delaroche, B. Aussedat, S. Aubry, G. Chassaing, F. Burlina, G. Clodic, G. Rard Bolbach, S. Lavielle and S. Sagan, *Anal. Chem.*, 2007, **79**, 1932–1938.
29 J. Ye, S. A. Fox, M. Cudic, E. M. Rezler, J. L. Lauer, G. B. Fields, A. C. Terentis and B. Raton, *J. Am. Chem. Soc.*, 2009, **132**, 980–988.
30 C. K. Payne, S. A. Jones, C. Chen and X. Zhuang, *Traffic*, 2007, **8**, 389–401.
31 M. Belting, *Trends Biochem. Sci.*, 2003, **28**, 145–151.
32 U. Häcker, K. Nybakken and N. Perrimon, *Nat. Rev. Mol. Cell Biol.*, 2005, **6**, 530–541.
33 S. Vannucchi, M. Ruggiero and V. Chiarugi, *Biochem. J.*, 1985, **227**, 57–65.
34 E. K. Nyren-Erickson, M. K. Haldar, J. R. Totzauer, R. Ceglowski, D. S. Patel, D. L. Friesner, D. K. Srivastava and S. Mallik, *Langmuir*, 2012, **28**, 16115–16125.
35 I. D. Alves, N. Goasdoué, I. Correia, S. Aubry, C. Galanth, S. Sagan, S. Lavielle and G. Chassaing, *Biochim. Biophys. Acta, Gen. Subj.*, 2008, **1780**, 948–959.
36 A. Nagarajan, P. Malvi and N. Wajapeyee, *Front. Endocrinol.*, 2018, **9**, 1–11.
37 S. C. H. A. Van Der Steen, A. A. G. Van Tilborg, M. J. E. Vallen, J. Bulten, T. H. Van Kuppevelt and L. F. A. G. Massuger, *Gynecol. Oncol.*, 2016, **140**, 527–536.
38 I. D. Alves, C. Bechara, A. Walrant, Y. Zaltsman, C. Y. Jiao and S. Sagan, *PLoS One*, 2011, **6**, e24096.
39 L. Bechtella, E. Chalouhi, P. Milán Rodríguez, M. Cosset, D. Ravault, F. Illien, S. Sagan, L. Carlier, O. Lequin, P. F. J. J. Fuchs, E. Sachon and A. Walrant, *ACS Chem. Biol.*, 2022, **17**, 1427–1439.
40 J. M. Tarbell and L. M. Cancel, *J. Intern. Med.*, 2016, **280**, 97–113.
41 I. Brockhausen, F. Vavasseur and X. Yang, *Glycoconj. J.*, 2001, **18**, 685–697.
42 H. Hauser, M. C. Phillips, B. A. Levine and R. J. P. Williams, *Nature*, 1976, **261**, 390–394.
43 M. Krumbiegel and K. Arnold, *Chem. Phys. Lipids*, 1990, **54**, 1–7.
44 A. Satoh, T. Toida, K. Yoshida, K. Kojima and I. Matsumoto, *FEBS Lett.*, 2000, **477**, 249–252.
45 G. P. Szekeres, S. Krekic, R. L. Miller, M. Mero, K. Pagel and Z. Heiner, *Phys. Chem. Chem. Phys.*, 2021, **23**, 13389–13395.
46 W. Y. C. Huang, S. G. Boxer and J. E. Ferrell, *Proc. Natl. Acad. Sci. U. S. A.*, 2024, **121**, e2319491121.